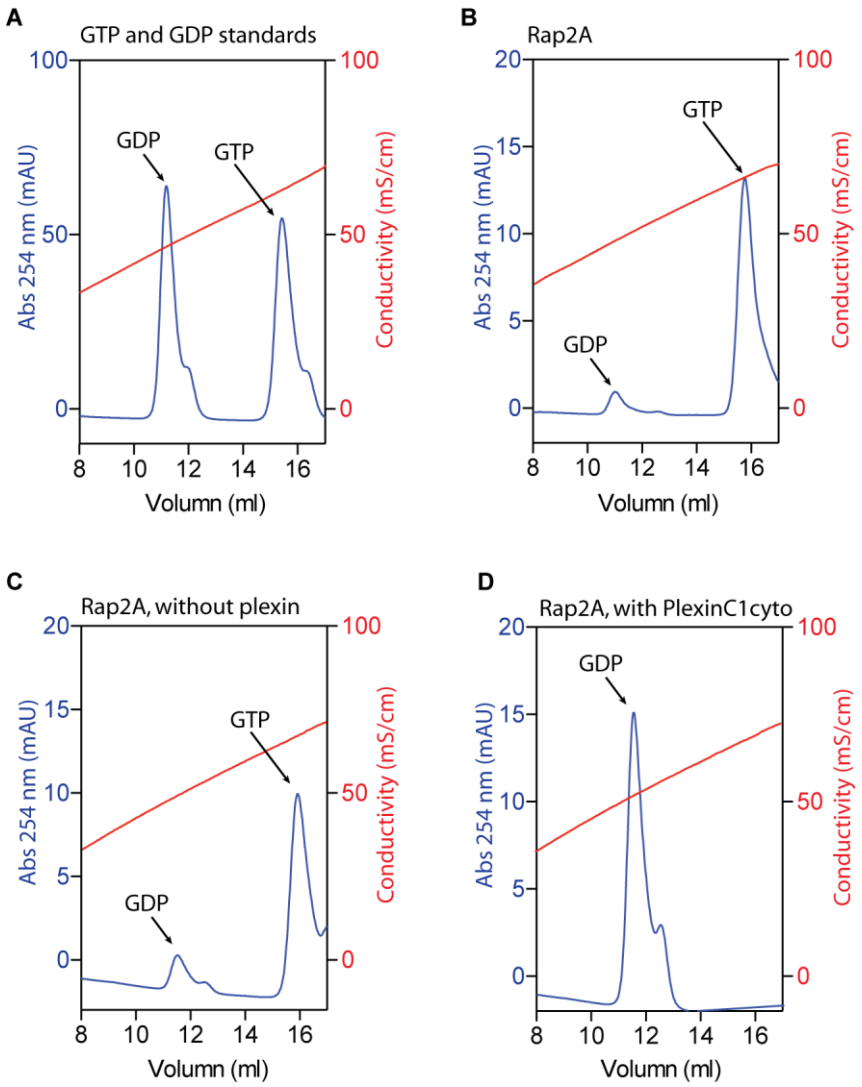

Figure S1. HPLC-based assay for plexin RapGAP activity.

(**A**) Anion exchange chromatogram of GDP and GTP standards. GDP and GTP are eluted at conductivities of ~40 mS/cm and ~60 mS/cm, respectively.

(**B**) Rap2A purified from *E. Coli.* is ~90% GTP bound, perhaps due to its low intrinsic GTPase activity.

(**C**) Incubation of Rap2A at room temperature for 30 min does not change the GTP/GDP ratio.

(**D**) Incubation of Rap2A in the presence of $PlexinC1_{cyto}$ at room temperature for 30 min leads to complete hydrolysis of bound GTP to GDP.

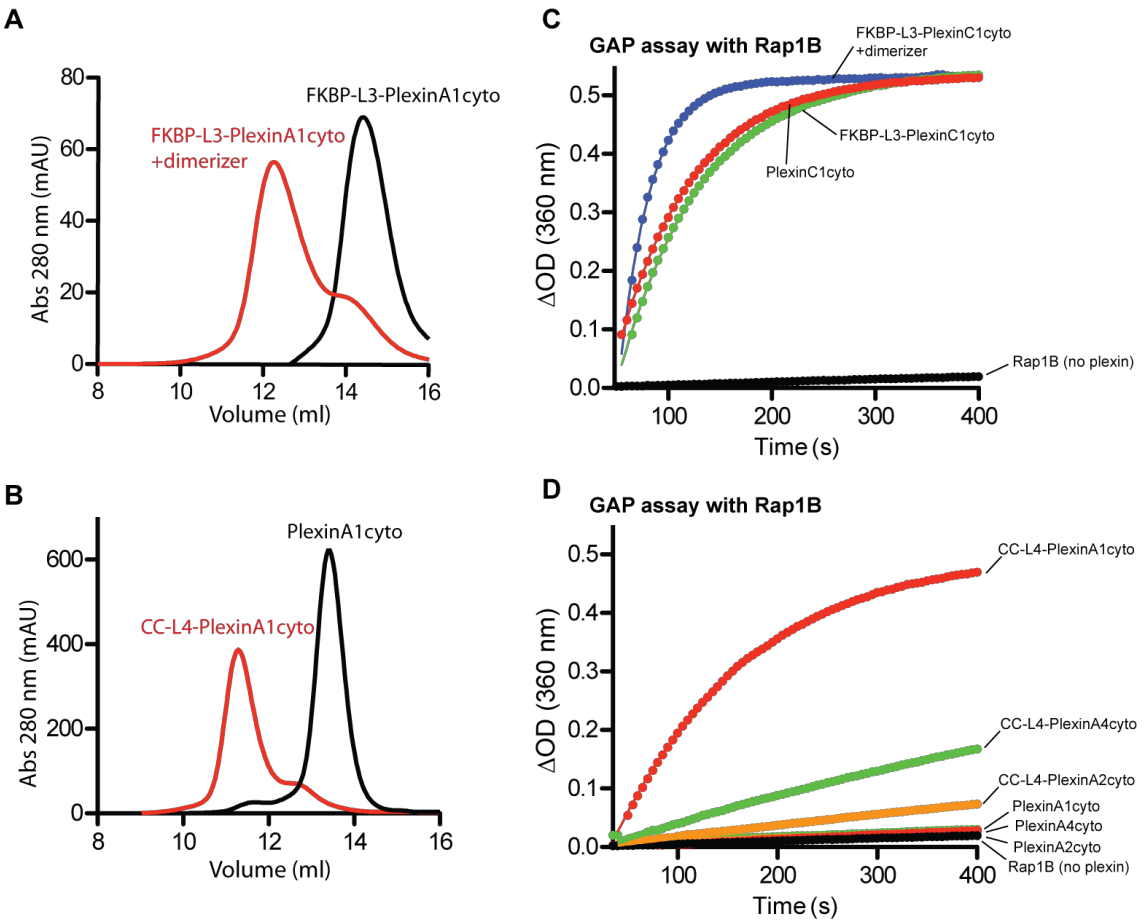

Figure S2. The RapGAP activity of plexins$_{cyto}$ is stimulated by induced dimerization.

(**A**) Gel filtration profiles of FKBP-L3-PlexinA1$_{cyto}$ with or without the dimerizer AP20187. (**B**) Gel filtration profiles of native PlexinA1$_{cyto}$ and CC-L4-PlexinA1$_{cyto}$. The results in (A) and (B) show that PlexinA1$_{cyto}$ is predominantly monomeric in solution, but can be induced to dimerize through the FKBP/AP20187 system or the coiled-coil dimerizer. The peak positions in (A) and (B) are not comparable because different columns were used.

(**C**) Stimulation of the RapGAP activity of FKBP-L3-PlexinC1$_{cyto}$ by dimerization.

(**D**) Coiled-coil enforced dimerization increases the RapGAP activity for PlexinA1$_{cyto}$, PlexinA2$_{cyto}$, and PlexinA4$_{cyto}$. CC-L4-PlexinA1$_{cyto}$ displays the highest degree of activation (28-fold). CC-L4-PlexinA2$_{cyto}$ and CC-L4-PlexinA4$_{cyto}$ are 3-fold and 8-fold more active than their respective native proteins. The GAP assay conditions are the same as in Fig. 1. Data shown are representative of at least 3 independent experiments.

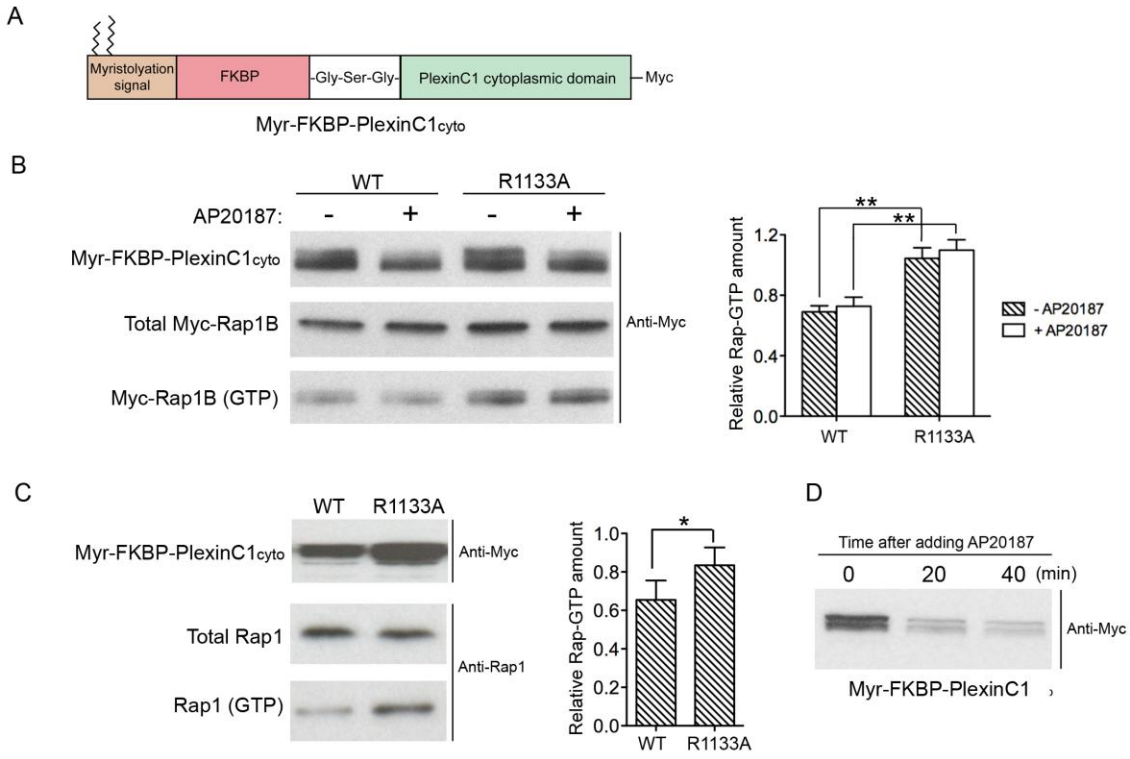

Figure S3. GST-RalGDS pull-down assays for plexin RapGAP activity in cells.

(**A**) Diagram of the construct of the membrane-localized FKBP-L3-PlexinC1$_{cyto}$ (named Myr-FKBP-PlexinC1$_{cyto}$). The myristoylation signal from the kinase Yes (residues 1-11) was fused to the N-terminus of FKBP-L3-PlexinC1$_{cyto}$ to target the protein to both plasma membrane and intracellular membranes.

(**B**) GST-RalGDS pull-down assays for transfected Myc-tagged Rap. Myc-tagged Rap1B was cotransfected with either the wild-type (WT) or the catalytically dead mutant (R1133A) of Myr-FKBP-PlexinC1$_{cyto}$ into HEK293T cells. The GST-RalGDS pull-down assay was employed to determine the amount of GTP-bound Myc-Rap1B, which was normalized to the amount of total Myc-Rap1B to calculate the relative Rap-GTP amount. Cells expressing wild-type PlexinC1 show significantly lower amounts of GTP-bound Rap1B compared with those expressing the R1133A mutant ($p<0.01$ by two-way ANOVA followed by Bonferroni post-hoc test, n = 5 experiments). Stimulation with AP20187 (the dimerizer) did not cause significant change in the amounts of GTP-bound Rap1B ($F_{1,16}=0.54$, $p=0.47$ by two-way ANOVA, n = 5 experiments). This lack of change could be because AP20187 treatment caused rapid loss of the plexin protein [shown in both (B) and (D)], and the ~3-fold increase in the RapGAP activity of FKBP-PlexinC1$_{cyto}$ as shown by our in solution assays (fig. S2C) is offset by the loss of the plexin protein.

Western blots were quantified using ImageJ. Error bar: standard error of the mean. Asterisks (**) indicate statistical significance ($p<0.01$).

(**C**) GST-RalGDS pull-down assays for endogenous Rap1 in HEK293T cells. The pull-down experiments and data analysis were performed as in (B), and an anti-Rap1 antibody (BD Transduction) was used for probing endogenous Rap1. Cells expressing the wild-type PlexinC1 have decreased amounts of GTP-bound endogenous Rap1 compared to those expressing the R1133A mutant. Error bar: standard error of the mean. Western blots were quantified using ImageJ. Asterisk (*) indicates statistical significance ($p<0.05$ by Student's t-test, n = 5 experiments).

(**D**) Loss of the expressed Myr-FKBP-PlexinC1$_{cyto}$ protein after AP20187 stimulation. The lower band likely corresponds to the N-terminally partially degraded protein because the Myc-tag is at the C-terminus. The rapid loss of the protein after AP20187 treatment is likely due to degradation as well, the mechanism of which is not understood at present.

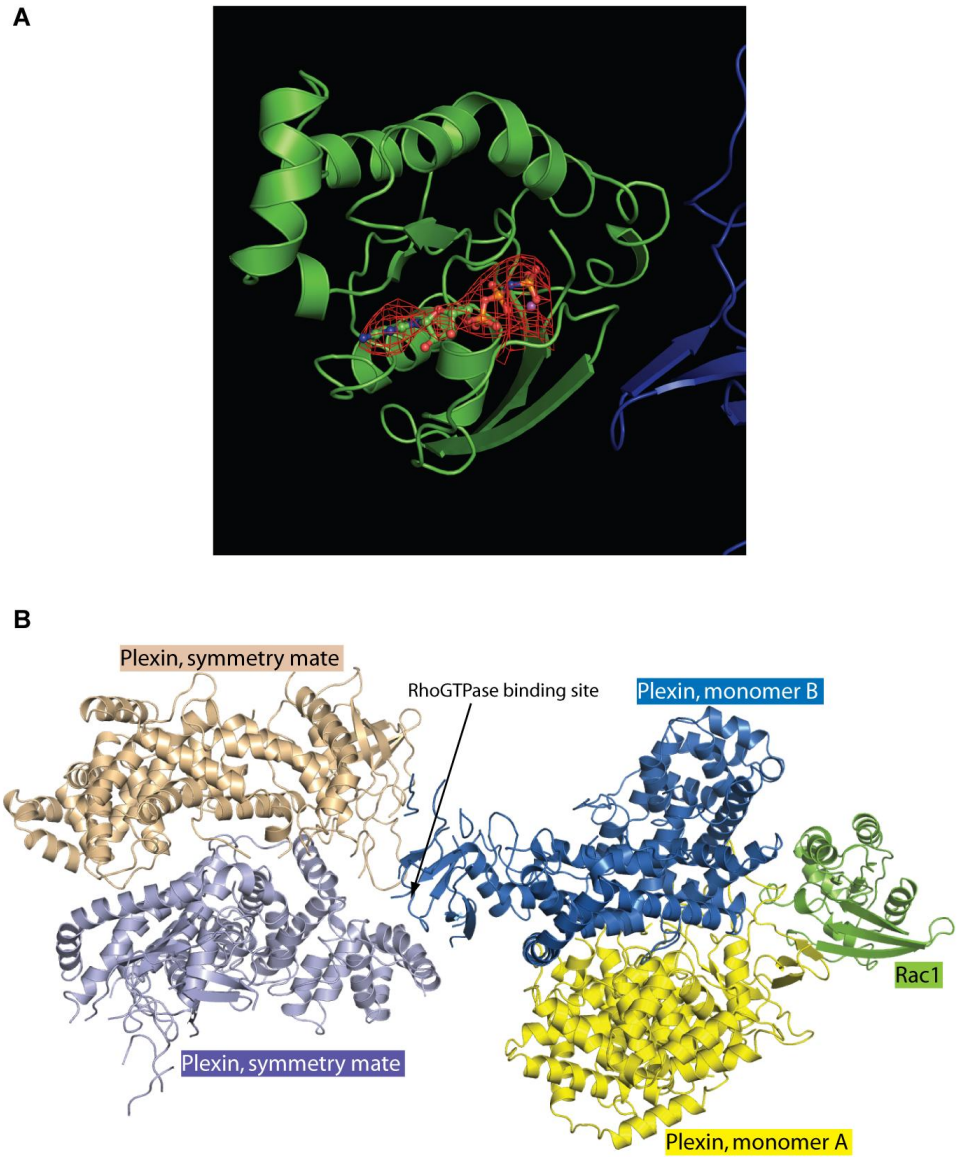

Figure S4. Crystal structure of the PlexinA1$_{cyto}$-Rac1 complex.

(**A**) Electron density showing the presence of GMP-PNP/Mg^{2+} at the nucleotide-binding site in Rac1. The GMP-PNP/Mg^{2+} molecules in the final refined model are shown as a stick-and-ball model. Rac1 and plexin (partially shown) are colored in green and blue, respectively. The (F_o - F_c) electron density contoured at 3σ (red) was calculated prior to including GMP-PNP/Mg^{2+} in the model.

(**B**) Molecular packing in the crystal. The asymmetric unit contains two plexin monomers. Monomer A (yellow) is bound to Rac1 (green), whereas the binding site in monomer B (blue) is empty. The space between the RhoGTPase binding site of monomer B and two symmetry related plexin molecules is too small to accommodate Rac1.